DOI: 10.1002/adem.200980045

In Vitro Biocompatibility of n-Type and Undoped Silicon Nanowires**

By *Bora Garipcan[+], Sedat Odabas[+], Gokhan Demirel, Joan Burger, Stephen S. Nonnenmann, Michael T. Coster, Eric M. Gallo, Bahram Nabet, Jonathan E. Spanier** and *Erhan Piskin**

The biocompatibility of undoped and n-type silicon nanowires (SiNWs), synthesized by metal-catalyzed chemical vapor deposition, was investigated in vitro, *and compared with that for SiO_2-coated silicon wafers. In cell interaction studies, L929 mouse fibroblast cells were used, in which MTT assay, AO/PI dye staining, cell proliferation/growth, and changes in cell adhesion/morphology on the surfaces were applied and investigated. Heamocompatibility of these materials were also tested. No significant cytotoxic effects were observed for either the undoped or for the n-type phosphorus-doped SiNWs. The cells on the nanowires exhibit high viability, normal nuclear, and morphological structure. They have shown no considerable negative blood response with respect to the control.*

Silicon nanowires (SiNWs) have found a wide range of applications in the field of electronics and optics due to their unique chemical and physical properties.[1–3] The amorphous SiO_x sheath on single crystalline silicon core allows various chemical modifications on SiNWs that are relevant for chemical and biological sensor applications.[4–6] Apart from the application of SiNW-based transistors for the selective detection of biomolecules, relatively little has been reported on the biocompatibility of SiNWs that is necessary for evaluating potential applications of SiNWs as a biomaterial. SiNWs can be considered as a biomaterial because it possesses advantages over other inorganic materials such as polycrystalline metals[7] and significantly, the degradation products of Si nanomaterials are metabolically tolerant in vivo and are found mainly in the form of $Si(OH)_4$.[7,8] Nagesha *et al.*[7] have shown SiNW surface under influence of an electrical bias exhibits an interfacial behavior that promotes calcification in stimulated plasma and have demonstrated non-cytotoxic behavior using human kidney fibroblast cells. Popat *et al.*[9] have investigated improved osteoblast performance by using controlled SiNW structures. Also, Kim *et al.*[10] demonstrate in vitro proliferation of mammalian cells on SiNW surfaces. However, Qi *et al.*[11] have demonstrated cytotoxic effect of SiNW suspensions on HepG2, human hepatocellular carcinoma cell line. Tunable dopant-induced carrier transport properties of SiNWs may allow the usage of doped SiNW nanostructures as cell guidance and cell adhesion for neurons and osteoblasts where electrical activity has an important role.[12–14] Also, these structures consisting of arrays of nanowire field-effect transistors integrated with the individual axons and dendrites of live mammalian neurons can be used for spatially resolved, highly sensitive detection, stimulation, and/or inhibition of neuronal signal propagation.[13] In addition, Hällström *et al.*[15]

[*] *Prof. E. Piskin, Dr. B. Garipcan, Dr. S. Odabas, Dr. G. Demirel*
Department of Chemical Engineering and Bioengineering Division, and Biyomedtek Beytepe, Hacettepe University, Ankara 06800, Turkey
E-mail: piskin@hacettepe.edu.tr
Dr. J. Burger, Dr. S. S. Nonnenmann, Dr. M. T. Coster, Dr. E. M. Gallo, Dr. B. Nabet, Dr. J. E. Spanier
Department of Materials Science and Engineering, Drexel University, Philadelphia, PA 19104, USA
[+] *Both authors contributed equally to this work*

[**] *Gokhan Demirel was supported as a post-doctoral fellow by The Scientific and Technological Research Council of Turkey (TUBITAK). Prof. Dr. Erhan Piskin was supported by Turkish Academy of Sciences (TUBA) as a full member. Jonathan Spanier acknowledges partial support for this work from the US Army Research Office (ARO) Materials Sciences Division, under YIP Award No. W911NF-04-1-0308 and from the Defense University Research Instrumentation Program (DURIP) Award No. W911NF-06-1-0127, and from the Department of Health of the Commonwealth of Pennsylvania.*

have investigated the interaction of GaP nanowires with mammalian neurons. On the other hand, with the increasing interest of using these materials in the field of clinic, researchers are also studying on in vivo biological systems. Linsmeier *et al*.[16] have investigated the brain-tissue response to nanowire implantations on rat model. In this study the in vitro biocompatibility properties of SiNWs (both undoped and n-type phosphorus-doped) prepared by Au nanocluster-catalyzed chemical vapor deposition (CVD) were investigated.

Experimental

Synthesis of Silicon Nanowires

The SiNWs were grown in a flowing precursor furnace via Au-catalyzed CVD on Si(100) possessing a 200-nm thick SiO_x layer. Here, 20 nm diameter Au colloids (Ted Pella, USA) were cast on poly-L-lysine-functionalized (in order to promote adhesion of the metal colloid in part due to its electrostatic charge and to reduce the agglomeration) SiO_x-coated Si(100) substrates, and the substrates were subsequently exposed to flowing precursor of 10% SiH_4 in H_2 (50 sccm) and carrier gas of N_2 ($\approx$ 50 sccm) at 500 °C under $\approx$ 75 Torr in a quartz tube furnace for 5 min. The furnace temperature was then briefly reduced to 480 °C and synthesis continued at the same parameters for another 20 min. In selected sets of SiNWs, introduction of phosphorus in the SiNWs as an n-type dopant was achieved with phosphine (PH_3): After synthesis of undoped SiNWs as described above, the SiNW-coated substrates were exposed to flowing precursor of 100 ppm PH_3 in H_2 (10 sccm) and carrier gas of N_2 ($\approx$ 50 sccm) at 575 °C under $\approx$ 75 Torr for 10 min. Finally, the post-doped SiNW-coated substrates were then annealed by increasing the temperature to 850 °C in the presence of carrier gas of N_2 ($\approx$ 50 sccm) under $\approx$ 75 Torr. The resulting post-phosphorus-doped and plain SiNWs were characterized by scanning electron microscopy (LEO-435 VP, England and Amray 1850FE).

In order to confirm the incorporation of dopant within the SiNWs, electrical contacts to randomly selected sample of undoped and doped SiNW growth product (dispersed on 200-nm thick SiO_2 film as gate oxide on a p-type Si(100) substrate) were produced via electron-beam lithography, thermal evaporation of an adhesion layer of Ni($\approx$ 5 nm) and a capping layer of Au ($\approx$ 200 nm), and subsequent rapid thermal annealing. Transconductance of undoped and doped SiNWs were measured with source-drain voltages ranging from $-5\,V < V_{sd} < 5\,V$ and gate voltages from $0 < V_g < +25\,V$ at room-temperature in vacuum (Lakeshore Cryotronics TTP4).

Cellular Interactions

MTT Assay.

The cytotoxicity of the SiNWs synthesized in the previous step was investigated by MTT assay using L929 mouse fibroblast cells [17]. Briefly, 1×10^4 cells well^{-1} were seeded on 96-well plates containing DMEM-F12, 10% FBS and 0.5% penicillin/streptomycin antibiotic solution. Cells were exposed to the Si wafer and to wafers containing undoped and doped SiNWs for $\approx$ 48 h at 37 °C in 5% CO_2. In order to determine the cell viability with respect to the control group (tissue culture flask), freshly prepared 13 μl sterile MTT solution and 100 μl fresh medium were added to each well. Following 3 h incubation at 37 °C in 5% CO_2, the medium was discarded and 100 μl fresh acidic isopropanol (0.04 N HCL) added to each well and mixed gently in order to solubilize the formazan crystals. The absorbencies were measured at 570 nm with a microplate reader (Biotek Instruments, USA).

AO/PI Dye Staining.

The assessment of the cytotoxicity by means of cell viability was made by using two florescent dyes, namely Acridine Orange (AO) and Propidium Iodide (PI).[18] Briefly, 5×10^4 cells well^{-1} were seeded on six well plates containing DMEM-F12, 10% FBS, and 0.5% penicillin/streptomycin antibiotic solutions. Cells were exposed to the Si wafer, and to the undoped and post-doped SiNWs for about 48 h at 37 °C in 5% CO_2 and the results are evaluated against control (tissue culture flask). For the staining, the medium was discarded and the cells were washed with sterile PBS. AO (25 μg ml^{-1}) and PI (25 μg ml^{-1}) solutions were prepared 1:1 v/v and interacted with the cells for 20 s. Subsequently, cells were washed with PBS for 10 s and mounted in PBS/Glycerol 1:1 v/v. Cells were observed under a fluorescence microscope (Olympus IX70, Japan).

Cell Proliferation/Growth.

Cell proliferation/growth was investigated by a trypan blue dye exclusion test in order to compare the growth of cells. Here, 1×10^4 L929 mouse fibroblast cells were seeded on the plates containing DMEM-F12, 10% FBS, and 0.5% penicillin/streptomycin antibiotic solutions and incubated at 37 °C in 5% CO_2 up to 5 d, in which they exposed to the Si wafer, as well as to undoped and doped SiNWs, and the results were evaluated against the plain tissue culture flask as control.

Cell Adhesion and Morphology.

Cell adhesion and morphology on the Si wafers and on undoped and doped SiNW-coated surfaces were investigated by using scanning electron microscopy (SEM). Using a procedure modified from Desai and coworkers [9], samples were placed into six-well plates and were sterilized under ultraviolet light in a laminar flow hood for 30 min. Cells were seeded at a concentration at 37 °C in 5% CO_2 for 24 h. Before imaging, the cells were fixed and dehydrated on Si wafers, and wafers containing doped, and alternately undoped SiNWs. Surfaces were rinsed twice in PBS, and then immersed in 3% glutaraldehyde (50% v/v, Sigma–Aldrich, USA) in PBS as a primary fixation solution. The cells were then dehydrated with increasing concentrations of ethanol (30, 50, 70, 90, and 100%) for 2 min in each solution. After dehydration of cells

with ethanol, the cells were dried and immersed in hexamethyldisilazane solution (Sigma–Aldrich, USA) for 5 min. The hexamethyldisilazane was removed, and the samples were air dried for 5 min. Samples were sputter-coated with gold and SEM imaging was performed on the LEO-435 VP SEM (UK).

Heamocompatibility Tests.

Prothrombin time (PT), activated partial thromboplastin time (APTT), and thrombin time (TT) and fibrinogen adsorption are well-known coagulation assays to determine the heamocompatibility of the material [19–21]. The anticoagulant activity of the Si wafer, and the undoped and doped SiNWs were evaluated by performing these assays using a semi-automatically START4 compact blood coagulation analyzer (Diagnostica Stago, France). All assays were tested using citrated human plasma from a healthy donor. PT, APTT, TT, and fibrinogen adsorption tests were performed as the following procedures: (i) *PT test*: the Si wafer, and the undoped and doped SiNWs were incubated with 50 μl citrated human plasma and 100 μl of prothrombin reagent for a minute (neoplatin®CI plus, Diagnostica Stago) in a transparent plastic tube at 37 °C; (ii) *APTT test*: 50 μl citrated human plasma was incubated with the Si wafer, and the undoped and doped SiNWs at 37 °C for 3 min. Fifty microliters of APTT reagent (C. K. Prest, Diagnostica Stago) was added, and the reaction mixture was incubated for another 3 min. The reaction was initiated by adding 50 μl of 0.025 M $CaCl_2$; (iii) *TT test*: 100 μl citrated human plasma was incubated with the Si wafer, and the undoped and doped SiNWs at 37 °C for 1 min, followed by the initiation of the reaction by adding 100 μl STA®Thrombin reagent; (iv) *fibrinogen adsorption test*: 100 μl citrated human plasma (diluted with PBS, 1:20) was incubated with the Si wafer, and the undoped and doped SiNWs at 37 °C for 1 min. Fifty microliters of fibrinogen reagent (Fibri-Prest®, Diagnostica Stago) was added, and fibrinogen adsorption was measured in mg ml^{-1}.

Results and Discussion

There are a number of factors that influence the electronic and photonic properties of SiNWs that can be controlled, including, e.g., control of nanowire diameter and wire morphology, crystal orientation, and impurity concentration. Specifically, introduction of hole acceptor and/or electron donor impurity atoms to SiNWs, resulting in p-type and alternatively, n-type conduction, is important for applications of SiNWs in nanoelectronics, and chemical and biochemical detection, and sensing.[22] Doping of SiNWs can be performed in several ways, including introduction during nanowire growth (*in situ*), or following growth (post-doping).[23] Diborane, trimethylboron, and PH_3 are gaseous compounds commonly used as dopants in a gas-phase synthesis of doped SiNWs through the so-called vapor–liquid–solid (VLS)-CVD method.[23–26] The post-doping process has advantages such as flexibility in the selection of the vapor-phase precursors for introducing dopant species and selective patterning of the doped SiNWs.[23] In our study we have applied the post-doping method and investigated the biocompatibility of the resulting doped SiNWs as compared with the as-grown undoped SiNWs. Our reasons for choosing post-doping and PH_3 as a dopant gas are the following: (i) to deposit higher amount of dopant on the outer SiO_x sheath of the SiNW which actually would interact with the surrounding environment (e.g., biological medium); and (ii) to evaluate the effects of elemental phosphorus especially on the cells, which is a toxic element itself, however a constituent of DNA, ATP, and many other biochemical molecules in the form of phosphates (PO_4^{3-}).[27]

Electronic Properties of n-doped Si Nanowires

Electronic carrier dopant type was verified and carrier concentration doping levels was determined for the post-doped SiNWs using room-temperature three-terminal electronic transport measurements. Plotted in Figure 1 is a representative family of traces of source-drain current versus source-drain bias voltage for an electrically contacted and doped SiNW at selected gate bias voltages ($0 < V_g < +25$ V). Carrier concentration n is obtained using $n = 1/(\rho e \mu_n)$, where $\rho = (IL/VA)^{-1}$ and where the electron mobility was found through the equation for transconductance, $dI/dV = \mu_n(C/L^2)$. Here the capacitance $C = (2\pi\varepsilon\varepsilon_o L)/[\ln(2h/r)]$, and ε is the relative dielectric constant of Si; L the wire length; h the thickness of the gate SiO_2 layer (=200 nm), and r the wire radius,[28] resulting in an estimated value for n of 1.51×10^{17} cm^{-3}, and an estimated mobility of $\mu_n = 0.232$ cm^2 $(V\,s)^{-1}$.

Interaction with Cells

The degree of possible cytotoxicity of the SiNWs was investigated by MTT assay and AO/PI dye staining. The data in Figure 2 indicate that percent cell viabilities were quite high

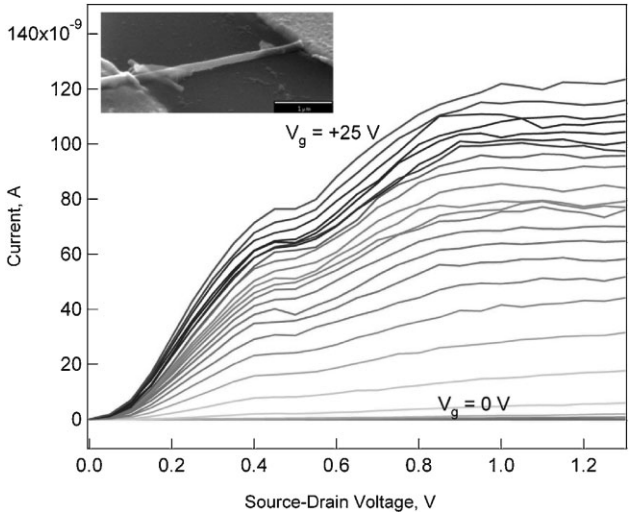

Fig. 1. Transconductance of PH_3-doped SiNW exhibiting n-type behavior. Plotted is the source–drain current as a function of source–drain bias, at selected values of gate bias voltage ($0 < V_g < +25$ V). The inset is a scanning electron micrograph image of the electrically contacted nanowire traversing an insulating gap between two Au contacts.

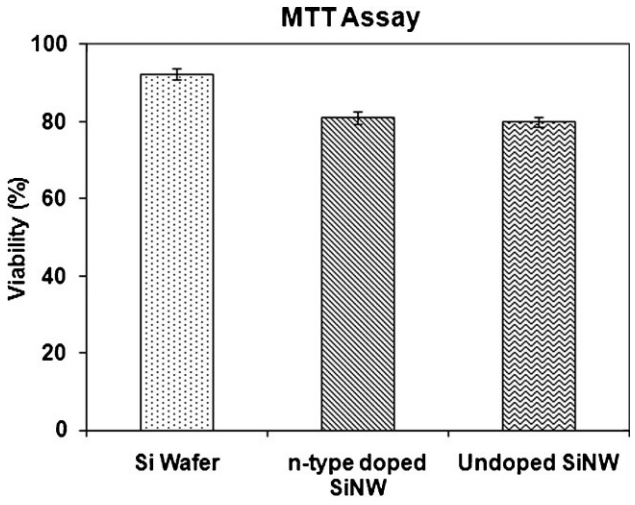

Fig. 2. Results of the MTT assay: Cell viabilities on the Si wafer, undoped, and n-type doped SiNW-coated substrates after 48 h exposure.

on all surfaces comparing to the control, in which the exposure time was 48 h. The highest viability was observed for the Si wafer, which was about 92%. Percent viabilities for the undoped and doped SiNWs were somewhat lower, at 80.04 and 81.10%, respectively.

In the AO/PI dye staining assay a mixture of AO and PI were used. Note that AO is a nucleic acid selective metachromatic stain useful for cell cycle determination and interacts with DNA and RNA by intercalation or electrostatic attraction, respectively. PI also binds DNA and the RNA by intercalation. Both dyes have fluorescence and can be observed under fluorescein and rhodamine filters. Representative images of the cells on the surfaces after 48 h of exposure are shown in Figure 3. No significant cytotoxic features were observed and almost all cells have a normal nuclear morphology on the control and the materials that investigated here (i.e., Si wafer, and undoped and doped SiNWs).

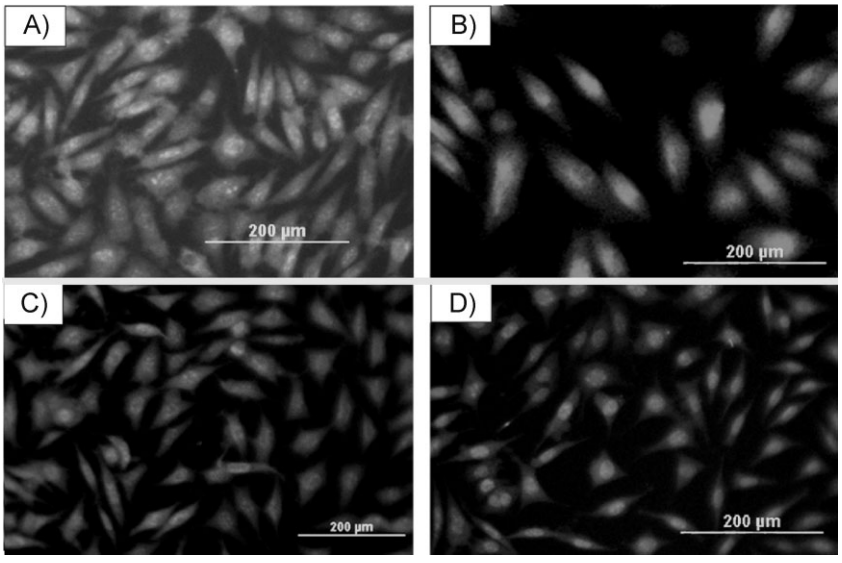

Fig. 3. Representative pictures of AO/PI dye stained of L929 mouse fibroblasts after 48 h exposure: (A) on the control; (B) on the silicon wafer; (C) on the undoped SiNWs; (D) on the n-type doped SiNWs.

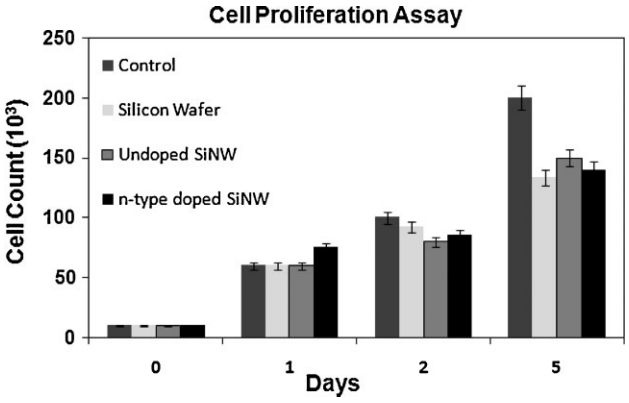

Fig. 4. Cell (i.e., L929 mouse fibroblasts) proliferation/growth on the control (tissue culture flask), silicon wafer, on undoped, and n-type doped SiNW-coated substrates.

Cell proliferation and growth was also examined in which L929 mouse fibroblast cells were allow to proliferate/grow on the test materials for up to 5 d. Changes of the cell counts in time on these surfaces are shown in Figure 4. We note that there were no significant adverse effects observed on the cells, and cells in all groups exhibited similar healthy proliferation patterns. We also note that slow proliferation rates because of insufficient free space or nutrients during the incubation are also an expected result when we compare Tissue culture flask as control with Nanowire surfaces.

Morphological differences of cells on the Si wafer, and undoped and doped SiNW surfaces were studied by SEM. Selected representative micrographs are presented in Figure 5. On the Si wafer surface, cells tend to spread on the smooth wafer surface and started to produce lamellae and numerous filopodia to adhere to the surface [Fig. 5(a)][29] On the undoped SiNW surfaces, cells have shown normal fibroblastic morphology and adherence [Fig. 5(b)]. On the surface coated with doped SiNWs, cells are seen to have started to spread and possess a more flattened morphology as compared with those on the undoped SiNW surface [Fig. 5(c)]. However, cells were still attaching to the surface by producing filopodia. The increased charge density of the doped SiNWs may result in instability of the charge distribution of the cell surface, thereby altering the morphology of the cells during adhesion.[22] Another factor is the influence of random topographies during the nanowire growth process.[30] Each SiNW-coated surface has randomly located nanowires and nanowire ensembles were prepared without precise control of nanowire diameters or their orientation with respect to the substrate. However, differences in the morphology of cells grown on surfaces possessing n-type doped SiNWs as compared with undoped SiNWs suggest that subtle differences, the different surface chemistry, and/or increased charged density

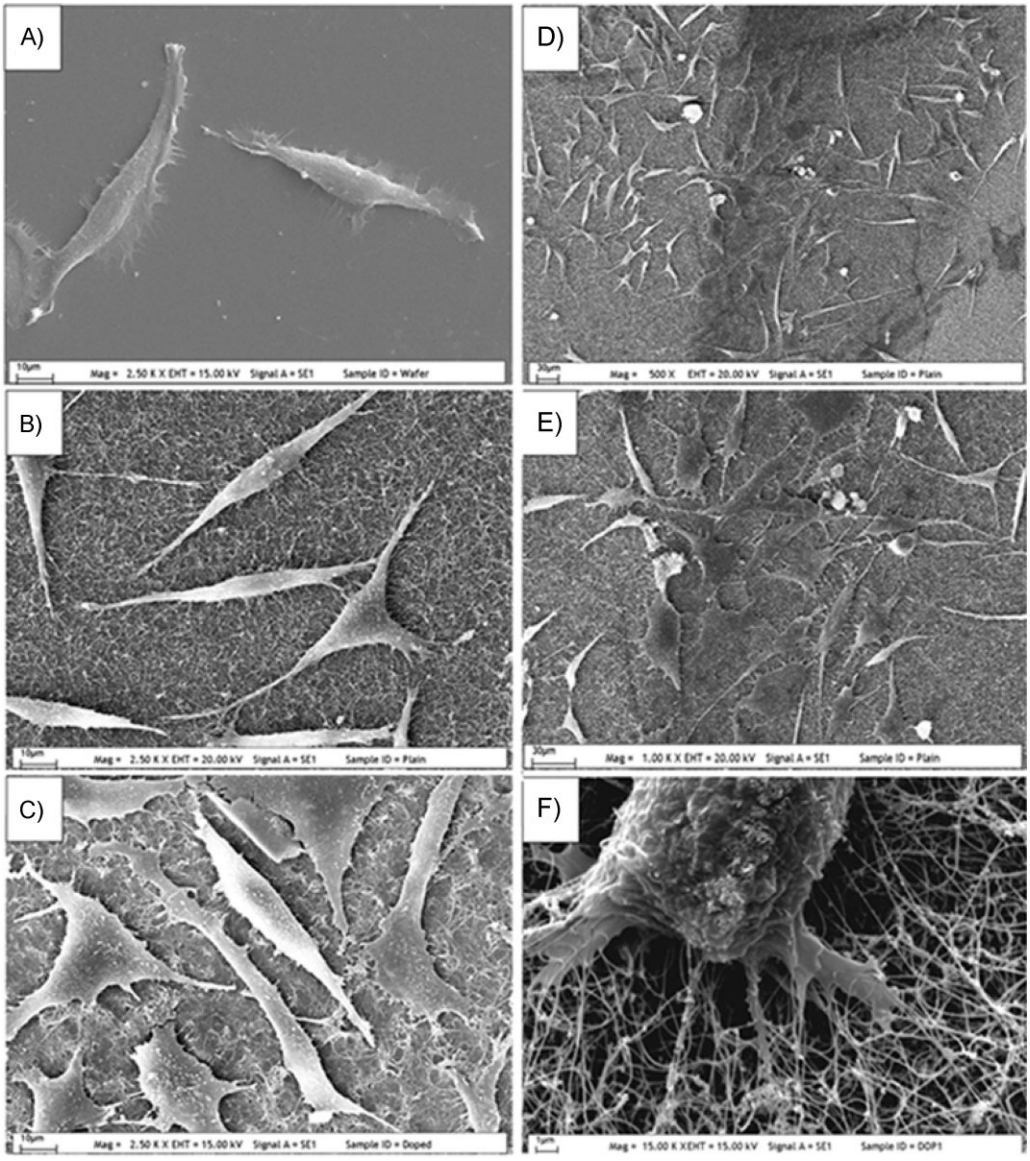

Fig. 5. Representative SEM images showing adhesion and morphology of L929 mouse fibroblasts: (A) Si wafer; (B) undoped SiNWs; (C) n-type SiNWs; (D) Effects of nanowire density on undoped SiNW surface (lower magnification); (E) Effect of nanowire density on undoped SiNW surface (higher magnification); (F) Interaction of n-type doped SiNWs with Fibroblast's filopodia.

can play an important role in controlling the nature of cell growth.

The effect of SiNW number density can be seen by the cell growth in a region where SiNWs have been dislodged and removed. This is obtained by scratching the substrate prior to and following the synthesis of the undoped SiNWs, resulting in higher and lower SiNW number densities, respectively, compared with the unscratched area (the rest of the substrate). Due to the increased number of interaction points with cells on high density areas, cells attached on the SiNW surface throughout their filopodia and kept their fibroblastic morphology. However, on the areas having a lower density of SiNWs, cells tended to spread more easily and possess more flattened morphologies [Fig. 5(d) and (e)]. On the nanotopographic surface of the doped SiNW surface, strong interactions between nanowires and the cell's filopodia were observed clearly in Figure 5(f).

Heamocompatibility

Fibrinogen adsorption, APTT, PT, and TT tests were widely used coagulation assays to determine the heamocompatibility of materials.[20,21] In this study, summarized in Table 1, these tests were performed to demonstrate the heamocompatibility of the undoped and doped SiNWs, where the bare Si wafer was also used for comparison. Note that coagulation times give the information about the heamocompatibility through intrinsic and extrinsic coagulation pathways.[31] As seen in Table 1, Si wafer and SiNWs have slightly higher coagulation times from the control.

Table 1. Heamocompatibility of the Si wafer, undoped, and doped SiNW-coated substrates

	PT [s]	ATTP [s]	TT [s]	Fibrinogen [mg ml^{-1}])
Control[a]	18.4 ± 0.2	53.0 ± 0.5	15.0 ± 0.3	325.4 ± 0.8
Si Wafer	18.8 ± 0.4	55.0 ± 0.4	15.9 ± 0.2	16.8 ± 0.3[b]
Undoped SiNWs	19.2 ± 0.3	56.4 ± 0.5	14.4 ± 0.4	14.1 ± 0.3[b]
n-type doped SiNWs	19.0 ± 0.3	53.5 ± 0.3	15.4 ± 0.2	16.1 ± 0.4[b]

[a] Control: Tissue culture polystyrene flask.
[b] The amount of fibrinogen adsorbed on the substrates.

Fibrinogen adsorption onto biomaterials surface is believed to play a major role in determining the heamocompatibility of the interested material because of its role in coagulation, and its ability to promote platelet adhesion.[32,33] Adsorption of fibrinogen from the blood is known to accelerate platelet adhesion and formation of thrombosis on foreign surfaces which show low binding amounts for fibrinogen are more biocompatible.[34–36] According to our results, the silicon wafer, the undoped, and the doped SiNWs have quite low fibrinogen adsorption values, demonstrating that they are quite heamocompatible. We note that on the fibrinogen column, first line is the amount of free fibrinogen in the plasma and others indicate the amount of adsorbed fibrinogen on the Si wafer, the undoped, and doped SiNW surfaces.

Conclusions

Silicon nanowires have found a wide range of applications in the field of electronics and optics due to their unique properties. Recently, researchers have started to attempt using these novel materials in biomedical applications, which brought questions about the biocompatibility concerns in sight. Here, in this study we synthesized SiNWs (both undoped and doped, following growth) and investigated their biocompatibilities in vitro by a series of tests. We tested also Si wafer as a substrate with a similar chemical composition for comparison. For the cell–material interaction studies, L929 mouse fibroblast cells were used and we investigated MTT viability, cell proliferation, AO/PI dye staining, and cell adhesion and morphology. The cells exhibited a very high viability and no significant cytotoxic features were observed as well as the control. The cells also showed relatively high fibroblastic morphology changes on the doped SiNW surface when compared to undoped SiNW surface. However, this morphological change does not adversely affect the viability, proliferation, and adhesion of the cells. Classical coagulation assays were performed to determine the preliminary heamocompatibility study of the doped and undoped SiNW surfaces. Surfaces have demonstrated no considerable negative blood response with respect to control group and have low fibrinogen adsorption properties. According these in vitro biocompatibility test results, we conclude that SiNWs may be considered as potential materials for biomedical applications, and that introduction of dopants, altering surface chemistry, and/or charge density may confer additional control in the growth and morphology of cells.

Received: November 5, 2009
Final Version: July 23, 2010

[1] D. D. D. Ma, C. S. Lee, F. C. K. Au, S. Y. Tong, S. T. Lee, *Science* **2003**, *299*, 1874.
[2] W. Lu, C. M. Lieber, *Nat. Mater.* **2007**, *6*, 841.
[3] L. Cao, B. Garipcan, S. Nonnenman, E. Gallo, B. Nabet, J. E. Spanier, *Nano Lett.* **2008**, *8*, 601.
[4] X. T. Zhou, J. Q. Hu, C. P. Li, D. D. D. Ma, C. S. Lee, S. T. Lee, *Chem. Phys. Lett.* **2003**, *369*, 220.
[5] F. Patolsky, G. Zheng, C. M. Lieber, *Nanomedicine* **2006**, *1*, 51.
[6] N. Chopra, V. G. Gavalas, B. J. Hinds, L. G. Bachas, *Anal. Lett.* **2007**, *40*, 2067.
[7] D. K. Nagesha, M. A. Whitehead, J. L. Coffer, *Adv. Mater.* **2005**, *17*, 921.
[8] S. H. C. Anderson, H. Elliott, D. J. Wallis, L. T. Canham, J. J. Powell, *Phys Status Solidi A* **2003**, *197*, 331.
[9] K. C. Popat, R. H. Daniels, R. S. Dubrow, V. Hardev, T. A. Desai, *J. Orthop. Res.* **2006**, *24*, 619.
[10] W. Kim, J. K. Ng, M. E. Kunitake, B. R. Conklin, P. Yang, *JACS* **2007**, *129*, 7228.
[11] S. J. Qi, C. Q. Yi, W. W. Chen, C. C. Fong, S. T. Lee, M. S. Yang, *ChemBioChem* **2007**, *8*, 1115.
[12] G. Zheng, W. Lu, S. Jin, C. M. Lieber, *Adv. Mater.* **2004**, *16*, 1890.
[13] F. Patolsky, B. P. Timko, G. Yu, Y. Fang, A. B. Greytak, G. Zheng, C. M. Lieber, *Science* **2006**, *313*, 1100.
[14] I. S. Kim, J. K. Song, Y. L. Zhang, T. H. Lee, T. H. Cho, Y. M. Song, et al., *Biochim. Biophys. Acta* **2006**, *9*, 907.
[15] W. Hällström, T. Mårtensson, C. Prinz, P. Gustavsson, L. Montelius, L. Samuelson, M. Kanje, et al., *Nano Lett.* **2007**, *7*, 2960.
[16] C. E. Linsmeier, C. N. Prinz, L. M. E. Pettersson, P. Caroff, L. Samuelson, J. Schouenborg, L. Montelius, N. Danielsen, *Nano Lett.* **2009**, *9*, 4184.
[17] T. Mossmann, *J. Immunol. Methods* **1983**, *65*, 55.
[18] H. L. Bank, *In Vitro Cell Dev. Biol.* **1987**, *24*, 266.
[19] F. Khan, L. M. Snyder, L. Pechet, *J. Thromb. Thrombolysis* **1998**, *5*, 83.
[20] S. Murugesan, T. J. Park, H. Yang, S. Mousa, R. J. Linhardt, *Langmuir* **2006**, *22*, 3461.
[21] J. Li, C. Cao, H. Zhu, *Diamond Relat. Mater.* **2007**, *16*, 359.
[22] M. Nolan, S. O'Callaghan, G. Fagas, J. C. Greer, T. Frauenheim, *Nano Lett.* **2007**, *7*, 34.
[23] B. K. Teo, X. H. Sun, *Chem. Rev.* **2007**, *107*, 1454.

[24] Y. Wang, K. K. Lew, T. T. Ho, L. Pan, S. W. Novak, E. C. Dickey, J. M. Redwing, T. S. Mayer, *Nano Lett.* **2005**, *5*, 2139.
[25] L. Pan, K. K. Lew, J. M. Redwing, E. C. Dickey, *J. Cryst. Growth* **2005**, *277*, 428.
[26] K. K. Lew, L. Pan, T. E. Bogart, S. M. Dilts, E. C. Dickey, J. M. Redwing, Y. Wang, M. Cabassi, T. S. Mayer, S. W. Novak, *Appl. Phys. Lett.* **2004**, *85*, 3101.
[27] J. Emsley, in *Nature's Building Blocks*, Oxford University Press, Oxford, England **2003**, 310.
[28] Y. Cui, X. Duan, J. Hu, C. M. Lieber, *J. Phys. Chem. B* **2000**, *104*, 5213.
[29] M. J. Dalby, S. Childs, M. O. Riehle, H. J. H. Johnstone, S. Affrossman, A. S. G. Curtis, *Biomaterials* **2003**, *24*, 927.
[30] S. G. Kumbar, M. D. Kofron, L. S. Nair, C. Laurencin, in *Biomedical Nanostructures* (Eds: K. E. Consalves, C. R. Halberstadt, C. T. Laurencin, L. S. Nair,) Wiley-VCH, Weinheim, Germany **2008**, Ch. 10, p. 261.
[31] A. Noyan, in *Physiology in Life and Medicine*, Meteksan Press, Ankara University, Turkey **2004**, 458.
[32] A. K. Bajpai, *J. Mater. Sci. Mater. Med.* **2008**, *19*, 343.
[33] W. B. Tsai, J. M. Grunkemeier, T. A. Horbett, *J. Biomed. Mater. Res.* **2003**, *67A*, 1255.
[34] G. A. Abraham, A. A. A. de Queiroz, J. S. Roman, *Biomaterials* **2002**, *23*, 1625.
[35] N. Kayirhan, A. Denizli, N. Hasirci, *J. Appl. Polym. Sci.* **2001**, *81*, 1322.
[36] S. R. Hanson, L. A. Harker, in *Biomaterials Science: An Introduction to Materials in Medicine* (Eds: B. D. Ratner, A. S. Hoffman, F. J. Schoen, J. E. Lemons,) Academic Press, San Diego, CA, USA **1996**, p. 193.

